Possible Half Metallic Antiferromagnet in a Hole-Doped Perovskite Cuprate Predicted By First-Principles Calculations

Yung-mau Nie and Xiao Hu

World Premier International Center for Materials Nanoarchitectonics (MANA), National Institute for Materials Science Tsukuba 305-0047, Japan

(Received 17 October 2007; revised manuscript received 7 November 2007; published 19 March 2008)

We formulate a scheme to realize a half metallic antiferromagnet (HMAFM), a material conductive in only one spin channel while exhibiting zero macroscopic magnetism, by doping carrier into a class of cuprates. The working rationale is exhibited as taking advantage of Hubbard repulsion of d electrons of Cu atoms and the charge-transfer effect from the associated O ligand to fully polarize the spin of a doped carrier. Specifically, doping one hole into the insulating ferrimagnet $Sr_8CaRe_3Cu_4O_{24}$ by replacing one of the eight Sr atoms by one Rb atom is predicted to achieve a HMAFM, presumably with room-temperature operation. Since the working rationale is the strong correlations of electrons commonly encountered in cuprates, it is expected that the present findings can shed light on a new way to develop a HMAFM.

DOI: 10.1103/PhysRevLett.100.117203 PACS numbers: 75.47.−m, 71.15.Mb, 71.27.+a, 75.50.Ee

Introduction.—Spintronic technologies, with potential advantages of speeding up data processing, reducing the power consumption, and increasing the circuit integration density, are rapidly booming [1–3]. The utmost key point to dominate the innovation of spintronics and to impose the research of new materials is how to efficiently manipulate the spin polarization of current. The half metal [4], i.e., which filters the current into a single spin channel without any external operation, fully meets this demand. To this day, all known half metallic materials are ferromagnetic, such as NiMnSb [5] and Co_2FeSi [6] of Heusler alloys, CrO_2 [7] of ferromagnetic metallic binary oxide, $La_{0.7}Sr_{0.3}MnO_3$ [8] and Fe_3O_4 [9] of the mixed-valence oxides, Sr_2FeMoO_6 [10] and $LaFeO_3$-$LaCrO_3$ superlattices [11] of double perovskites, zigzag graphene nanoribbons [12] of carbon-based nanostructures, and so on.

In fact, van Leuken and de Groot [13] have proposed a half metallic antiferromagnet (HMAFM) to achieve a completely spin-polarized current by a nonmagnetic material. In half metallic ferromagnets (HMFMs) the generation of the spin-polarized current is unavoidably restricted by the formation of magnetic domains as usually happening in ferromagnets; meanwhile, the stray field from a ferromagnet may be harmful in highly integrated circuits. All these drawbacks can be overcome if replacing HMFM by HMAFM systems.

The first proposed HMAFM is the $V_7MnFe_8Sb_7In$ alloy [13]. In order to facilitate the formation of stoichiometric HMAFM, Pickett [14] suggested applying simple-structural double perovskites to substitute the previous Heusler alloys. Possible HMAFMs of double perovskites by A-site replacement have been postulated, including $LaAVRuO_6$ (A = Ca, Sr, Ba) [15] and $ALaVMoO_6$ (A = Ca and Sr) [16]. In addition, Ködderitzsch *et al.* [17] and Akai and Ogura [18] proposed to realize HMAFM in a nonstoichiometric form by means of low-density vacancy defects in oxide insulators and dilute doping of transition-metal cations in semiconductors, respectively. Despite all these efforts, a definite confirmation of HMAFM is lacking at the time this was written.

In the present work, we propose to realize HMAFM by doping carrier into insulating cuprates. The magnetic moment $1\mu_B$ per unit cell of the state-of-the-art octuple-perovskite cuprate $Sr_8CaRe_3Cu_4O_{24}$ [Fig. 1(a)] inspires us to apply this scheme, noticing that the integral magnetic moment is the hallmark of a stoichiometric half metal. Since the total magnetization per unit cell is exactly equal to the spin moment of one electron, one doped hole, e.g., achieved by 1/8 replacement of the divalent Sr atoms by one univalent Rb atom, simultaneously compensates for the magnetism of the parent material and produces spin-polarized conduction electrons; it is thus able to achieve

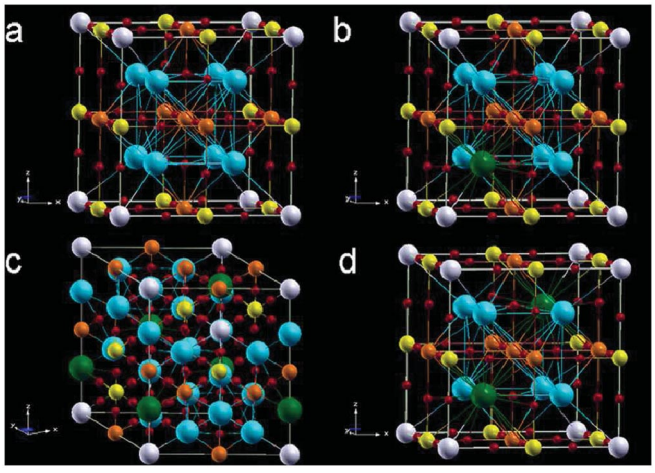

FIG. 1 (color). Schematic representation of the unit cell. (a) Parent material (space group: Pm-3m). Two unit cells for 1/8 replacement of Sr atoms by the Rb atom: (b) the lowest symmetric, and (c) the highest symmetric (space group: $R3m$). (d) The 1/4 replacement. The Sr (blue), Rb (green), Ca (gray), Re (yellow), Cu (brown), and O (red) atoms are shown in colored spheres.

HMAFM provided that the magnetic backbone of the Cu cations in the parent material is amenable to the doping. The above idea is manifested by first-principles calculations as detailed below. Based on the Hubbard repulsion between d electrons of Cu atoms and the charge-transfer effect from the associated O ligand, which generally exists in cuprates, the present strategy is expected to be applicable to a wide class of materials and thus to open a new way to generate HMAFM.

Methods.—First-principles calculations are performed within the scheme of DFT + U [19] with the generalized gradient approximation [20] of the exchange-correlation functional. The on-site Coulomb and exchange parameters are $U = 10$ and $J = 1.2$ eV for $3d$ states of the Cu atom as the previous calculations [21]. The all-electron full-potential projector augmented wave method [22,23] is implemented with the VASP package [24]. The cutoff energy of 400 eV for plane-wave bases, and a Γ-centered $8 \times 8 \times 8$ Monckhorst-Pack grid for k sampling are used. Starting from the measured structure parameters [25], the ionic relaxation is achieved upon the conjugate-gradients technique [24], and the lattice constants of minimal energy are determined via calculating the bulk modulus.

Before doping.—$Sr_8CaRe_3Cu_4O_{24}$ behaves as a Mott insulator and shows a ferrimagnetic ground state as depicted in Figs. 2 and 3(a) [21,25]. The magnetic moments are mainly contributed from Cu atoms. The distribution of the spin moment at Cu1, which is centered at a perfect O octahedron, is of the typical e_g-orbital shape. That at Cu2, which is centered at the O octahedron elongated in the xy plane due to the high valence of its second nearest neighboring Re^{+7} ion [21,26], is in the form of the $d_{3z^2-r^2}$ type of e_g orbital [27].

The spin moments of Cu1 and Cu2 are aligned antiparallel with the values of -1.05 and $0.74\mu_B$, respectively, via the well-known superexchange interaction. The ferrimagnetic spin configuration of Cu atoms, the absence of the spin moment of Re cations, as illustrated in Fig. 3(a), and the total magnetic moment of unit cell $1.0\mu_B$, respectively, agree well with the experimental evidences from the Cu-NMR spectra [28], electron energy-loss spectra [25,26], and the spontaneous magnetization at $T = 0$ [25]. Quantum Monte Carlo simulations [29] on the effective spin model of Cu cations reproduces well the critical temperature observed in the experiment [25], $T_c \sim 440$ K.

There are small spin moments ($\sim -0.08\mu_B$) on the O2 sites, located between Cu1 and Cu2, antiparallel to that of Cu2 [Fig. 3(a)]. The spin configuration of O2 sites can be interpreted as the result of the charge-transfer effect postulated by Zaanen *et al.* [30], i.e., charge fluctuations of the type $d^n \rightarrow d^{n+1}\mathbf{L}$ ($\mathbf{L}$ denotes a hole in the ligand anion valence band). The involvement of the charge-transfer effect in the strong correlations of the $3d$ electrons of Cu2, additionally to the on-site Coulomb repulsion, is evidenced by the difference between the Hubbard energy splitting $U \sim 11.5$ eV in Fig. 4(a) and the input value

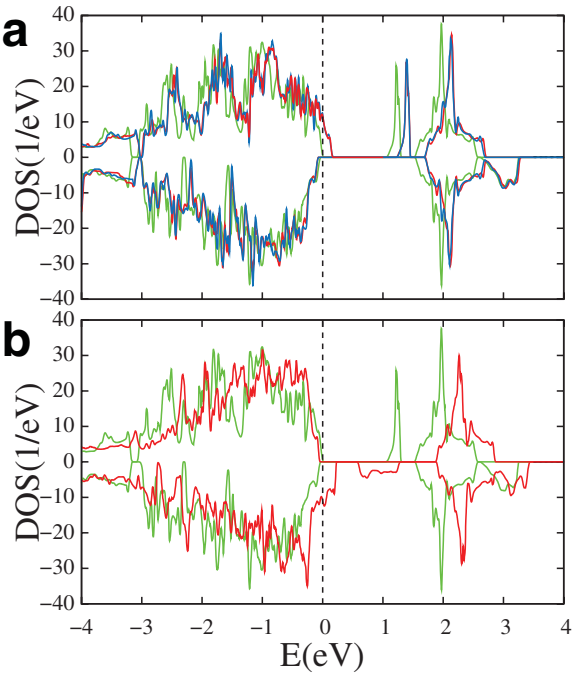

FIG. 2 (color). Total density of states. (a) Parent material (green) and 1/8 replacement with blue (red) for the highest (lowest) symmetric structure of the unit cell in Figs. 1(c) and 1(b). In order to exactly contrast with the results of parent material, hereafter the results for 1/8 replacement refer to the unit cell defined as Fig. 1(b) unless noted otherwise. (b) Parent material (green) and 1/4 replacement (red).

$U_{\text{eff}}(= 10\text{–}1.2) = 8.8$ eV [19,31]. Herein the charge-transfer energy Δ is estimated as ~ 6 eV [32] [Fig. 4(a)].

Contrarily, the resulting U of Cu1 is very close to U_{eff} [Fig. 4(a)], which indicates that little of the p-d hybridization is participating in the strong correlation of Cu1. The contrast between Cu1 and Cu2 with respect to the charge-transfer effect also leaves its footmark in the shapes of the isosurface of spin magnetization density [Fig. 3(a)], which clearly correspond to the orbital ordering (e_g versus $d_{3z^2-r^2}$) and the charge ordering (Cu^{3+} versus Cu^{2+}) discussed in Ref. [21].

Analogous to the concept of antiferromagnetic scattering of conduction electrons due to the local magnetic moment of the impurity in the Anderson model [30], the hopping $2p_z$ electrons of O sites with spin antiparallel to the Cu-site local moment will be energetically favored in the charge-transfer process, which reflects on the partial density of states of O2 $2p_z$ electrons [Fig. 4(a)]. Therefore, the spin moments at O2 tend to align themselves antiparallel to that of Cu2.

Critical doping.—DFT + U calculations reveal that the highest occupied bands are mainly made of $2p$ states of O2 sites in the original system. Doping hole(s) will therefore reduce the electron population in the O-$2p$ bands, analogous to the formation of the Zhang-Rice spin-singlet state for the high-temperature superconductivity [33].

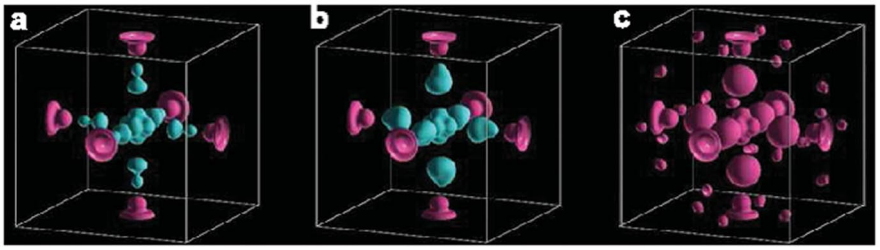

FIG. 3 (color). Isosurface of spin magnetization density at $\pm 0.07 \mu_B$ Å^{-3} [pink (blue) color: + (−) sign]. Here Cu1 locates at the center; Cu2 at the face center; O2 between Cu1 and Cu2. (a) Parent material, (b) 1/8 replacement, and (c) 1/4 replacement.

In the present study, we replace one of the eight Sr atoms by one Rb atom in order to achieve one-hole doping. In the same row of the periodic table, the Rb atom has a similar size to that of Sr, which ensures the hole-doped modification to preserve the structure of the parent material. Because of the high ionic character of Rb, we expect that the replacement will not disturb much the band structure. As a matter of fact, except for the localized states at −8.5 eV derived from Rb, the whole density of states remains a likely shape and all states shift upward to higher energies upon Rb replacement according to calculations [Fig. 2(a)]. The band structure of Cu sites and the ferrimagnetic spin moments of Cu1 and Cu2 (with the values of -1.06 and $0.74 \mu_B$) are completely preserved as illustrated in Figs. 4(b) and 3(b), respectively.

The e_g states of Cu1 with down-spin polarization induce a splitting in t_{2g} orbits via the intra-atomic Hund's coupling [Fig. 4(b)], which reduces the energy of p_x and p_y states of O2 with down spin through hybridization. At the O2 site the Hund's coupling due to the net local moment of p_z states also enhances the exchange splitting of the p_x and p_y states [34]. Therefore, the p_x and p_y orbits of O2 with up spin entirely respond to the reduction of the electron population caused by the hole doping, which increases the local moments of O2 up to -0.26 and $-0.16 \mu_B$ at the sites close and far from the doped Rb atom. As depicted in Figs. 2(a) and 4(b), it not only makes the up-spin channel (only) cross the Fermi level and thus achieves the half metallicity (with bandwidth of 0.25 eV) but also results in the magnetic moment per unit cell $\mu_{\text{tot}} = 0.00 \mu_B$ [35]. Namely, the loss of electron spin moment $1 \mu_B$ upon hole doping fully polarizes in the up-spin channel and exactly cancels out the $\mu_{\text{tot}} = 1 \mu_B$ in the parent system. The same results are obtained for both unit cells of $Sr_7RbCaRe_3Cu_4O_{24}$ [Figs. 1(b) and 1(c)].

Combining the complete spin cancellation and the metallic band structure in the single spin channel, it is concluded that the compound $Sr_7RbCaRe_3Cu_4O_{24}$ should be a new candidate of HMAFM. Since the backbone ferrimagnetic spin configuration of Cu atoms is sustained, the magnetic transition temperature for the present doped ma-

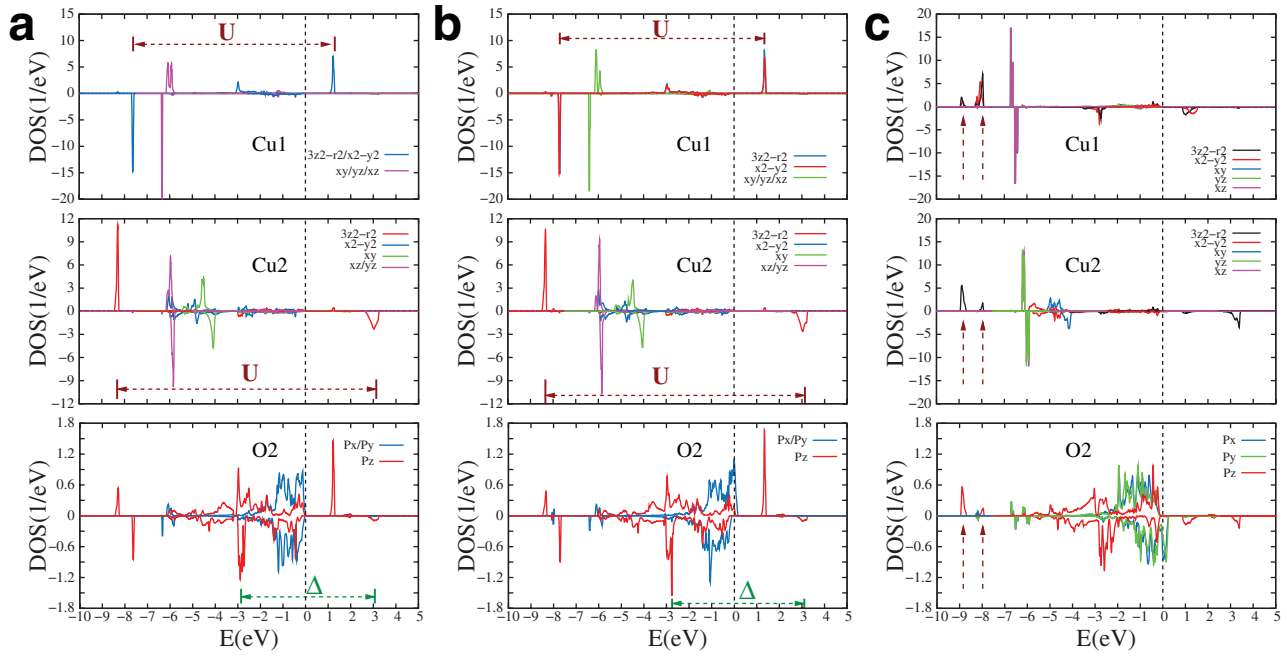

FIG. 4 (color). Partial density of states (PDOS) for the $3d$ states at the Cu1 and Cu2 sites, and the $2p$ states at the O2 site. (a), (b), and (c), respectively, depict the cases of the parent material, the 1/8 replacement, and the 1/4 replacement. In (b) the O2 atoms close to the Rb atom are displayed. The other O2 atoms show the similar half metallic features in the PDOS. In (c) the degenerate lower Hubbard states of Cu1 and Cu2, and the associated hybridization of O2 are highlighted by the arrow marks.

terial is expected to be comparable with that of the parent material.

Overdoping.—Hole doping can be carried out further by quarter replacement of Sr atoms by Rb atoms, i.e., $Sr_6Rb_2CaRe_3Cu_4O_{24}$. It turns out that the lower Hubbard bands of Cu1 and Cu2 now lie at the same energy levels as depicted in Fig. 4(c), and the spin moments on Cu1 and Cu2 align themselves ferromagnetically (with the magnitudes of 1.31 and $\sim 0.95\mu_B$, respectively) as exhibited in Fig. 3(c), in sharp contrast to the undoped and one-hole-doped cases. The ferromagnetic ground state is understood as follows: doping two holes sufficiently increases the population of mobile conduction electrons of O2 enough to eliminate the localization of individual lower Hubbard states of Cu1 and Cu2, and results in degenerate states. Under such a condition, the energetically preferential state exhibits a spatially antisymmetric wave function in order to reduce the Coulomb repulsion; Pauli's exclusion principle then imposes the ferromagnetic spin alignment.

The two holes reside on O2 sites and totally go to the down-spin channel to give a net local moment of O2 ($\sim 0.45\mu_B$), which leaves a finite DOS at the Fermi level [Fig. 4(c)]; as such $Sr_6Rb_2CaRe_3Cu_4O_{24}$ becomes half metallic as depicted in Fig. 2(b). A direct, ferromagnetic exchange interaction appears and makes the fully polarized spin state of $\mu_{\text{tot}} = 7\mu_B$ [see Fig. 3(c)]. Transition from an AFM insulator to a FM metal has been observed in other materials such as $La_{1-x}Sr_xMnO_3$ [36], with the mechanism being the double-exchange effect.

Summary.—Based on first-principles calculations, we have formulated a scheme to realize HMAFM by doping carrier into insulating cuprates. The working rationale is the *d-d* Hubbard repulsion of Cu atoms and the charge-transfer effect of O ligands, which fully polarize the spin of doped carrier. We propose explicitly a HMAFM $Sr_7RbCaRe_3Cu_4O_{24}$ by $1/8$ replacement of Sr atoms by one Rb atom in the insulating, ferrimagnetic parent compound. From the solid magnetic backbone of Cu atoms, the HMAFM is expected to work above room temperature. A further increase in the population of conducting $2p$ electrons of O atoms flips the spins of Cu sites to ferromagnetic and results in a HMFM. It is confirmed by the same calculations mentioned above that the same physics takes place when *K* is used instead of Rb. The interplay of the Hubbard interaction and the charge-transfer effect is frequently observed in late-transition-metal oxides. As such, the present scheme is heuristic for discovering more HMAFM in perovskite cuprates, to which attention was paid for searching high-T_c superconductivity in the past two decades.

The authors appreciate the discussions with X.-G. Wan and I. Solovyev. Calculations were performed on HITACHI-SR11000 in NIMS. X. H. is partially supported by the project ITSNEM of CAS. This work was supported by WPI Initiative, MEXT, Japan, and partially by the project ITSNEM of CAS.

[1] S. A. Wolf *et al.*, Science **294**, 1488 (2001).
[2] P. Grünberg *et al.*, Phys. Rev. Lett. **57**, 2442 (1986).
[3] M. N. Baibich *et al.*, Phys. Rev. Lett. **61**, 2472 (1988).
[4] R. A. de Groot *et al.*, Phys. Rev. Lett. **50**, 2024 (1983).
[5] C. T. Tanaka, J. Nowak, and J. S. Moodera, J. Appl. Phys. **86**, 6239 (1999).
[6] Z. Gercsi *et al.*, Appl. Phys. Lett. **89**, 082512 (2006).
[7] S. M. Watts *et al.*, Phys. Rev. B **61**, 9621 (2000).
[8] J. M. D. Coey, M. Viret, and S. von Monãr, Adv. Phys. **48**, 167 (1999).
[9] A. Yanase and K. Siratori, J. Phys. Soc. Jpn. **53**, 312 (1984).
[10] K.-I. Kobayashi *et al.*, Nature (London) **395**, 677 (1998).
[11] K. Ueda, H. Tabata, and T. Kawai, Science **280**, 1064 (1998).
[12] Y.-W. Son, M. L. Cohen, and S. G. Louie, Nature (London) **444**, 347 (2006).
[13] H. van Leuken and R. A. de Groot, Phys. Rev. Lett. **74**, 1171 (1995).
[14] W. E. Pickett, Phys. Rev. B **57**, 10613 (1998).
[15] J. H. Park, S. K. Kwon, and B. I. Min, Phys. Rev. B **65**, 174401 (2002).
[16] M. Uehara, M. Yamada, and Y. Kimishima, Solid State Commun. **129**, 385 (2004).
[17] D. Ködderitzsch *et al.*, Phys. Rev. B **68**, 125114 (2003).
[18] H. Akai and M. Ogura, Phys. Rev. Lett. **97**, 026401 (2006).
[19] A. I. Liechtenstein, V. I. Anisimov, and J. Zaanen, Phys. Rev. B **52**, R5467 (1995).
[20] J. P. Perdew, K. Burke, and M. Ernzerhof, Phys. Rev. Lett. **77**, 3865 (1996).
[21] X. Wan, M. Kohno, and X. Hu, Phys. Rev. Lett. **94**, 087205 (2005); *ibid.***95**, 146602 (2005).
[22] P. E. Blöchl, Phys. Rev. B **50**, 17953 (1994).
[23] G. Kresse and D. Joubert, Phys. Rev. B **59**, 1758 (1999).
[24] G. Kresse and J. Furthmüller, Comput. Mater. Sci. **6**, 15 (1996).
[25] E. Takayama-Muromachi *et al.*, J. Solid State Chem. **175**, 366 (2003).
[26] M. Isobe *et al.*, J. Magn. Magn. Mater. **312**, 131 (2007).
[27] In perovskite cuprates that become superconducting at unconventionally high temperatures upon carrier doping, the spin moment is subjected by the $d_{x^2-y^2}$ orbital of Cu centered at the O octahedron elongated along the z axis.
[28] Y. Uchida, M. Isobe, and E. Takayama-Muromachi, J. Magn. Magn. Mater. **272–276**, 818 (2004).
[29] M. Kohno, X. Wan, and X. Hu, J. Phys. Soc. Jpn. Suppl. **74**, 98 (2005).
[30] J. Zaanen, G. A. Sawatzky, and J. W. Allen, Phys. Rev. Lett. **55**, 418 (1985).
[31] V. I. Anisimov *et al.*, Phys. Rev. B **48**, 16929 (1993).
[32] M. Imada, A. Fujimori, and Y. Tokura, Rev. Mod. Phys. **70**, 1039 (1998).
[33] F.-C. Zhang and T. M. Rice, Phys. Rev. B **37**, 3759 (1988).
[34] I. S. Elfimov *et al.*, Phys. Rev. Lett. **98**, 137202 (2007).
[35] The summation of local moments on Cu1, Cu2, and O2 $-1.05 + 0.74 \times 3 - 0.26 \times 3 - 0.16 \times 3 = -0.09\mu_b$ is slightly different from the integration in unit cell $0.00\mu_B$ due to other small contributions below the cutoff value of Fig. 3.
[36] Y. Okimoto *et al.*, Phys. Rev. Lett. **75**, 109 (1995).